



Developing a Saturation Height Function (SHF) for the classified Hydraulic Flow Unit, a case study from the Middle Miocene Carbonate reservoir in the Song Hong Basin, Vietnam



Dung Trung Nguyen ^{1,*}, Man Quang Ha ¹, Viet Hong Nguyen ², Huong Thien Phan ³,
Cu Minh Hoang ¹, Hoa Khac Truong ¹

¹ Petrovietnam Exploration Production Corporation, Hanoi, Vietnam

² Schlumberger Vietnam, Hochiminh, Vietnam

³ Hanoi University of Mining and Geology, Hanoi, Vietnam

ARTICLE INFO

Article history:

Received 20th July 2023

Revised 26th Oct. 2023

Accepted 21st Nov. 2023

Keywords:

Carbonate reservoir,
Hydraulic flow unit,
Saturation height function,
Southern part of Song Hong
basin,
Water saturation.

ABSTRACT

The Middle Miocene carbonate is the main gas bearing reservoir in the southern part of the Song Hong basin. Carbonate reservoirs present challenges for engineers and geologists to characterize because of their complexity due to depositional and diagenetic processes. The log based calculated water saturation S_w for this complex carbonate reservoir bears a lot of uncertainties due to its heterogeneity that strongly affects to m and n values in the water saturation equation. As the calculated S_w strongly affects the Hydrocarbon Initially In Place (HIIP) estimation, the production performance prediction, etc., the alternative method using the Saturation Height Function (SHF) based on the capillary pressure was introduced. The SHF building process uses the combination of the result of HFU classification and permeability prediction given by machine learning methods, which have become a very useful tool for complex reservoir characterization such as carbonate reservoir for decades. Our obtained results allowed us to subdivide the carbonate reservoir into 5 Hydraulic Flow Unit (HFU) by using unsupervised machine learning methods, and then the capillary pressure (P_c) curves were classified and a proper saturation-height function using Skelt Harrison equation was assigned to individual HFU after testing with common SHF equations. The HFU number for each individual point was predicted based on the log data measured along the borehole using the supervised machine learning techniques while the S_w was calculated using the chosen SHF model and the FWL defined on log curves and pressure data from RCI measurement. The S_w computed from the SHF model is reliable and can be used for water saturation estimation for the whole field for known FWL and predicted HFU numbers.

Copyright © 2023 Hanoi University of Mining and Geology. All rights reserved.

*Corresponding author

E - mail: dungnt-tktdtn@pvep.com.vn

DOI: 10.46326/JMES.2023.64(6).01

1. Introduction

The CX gas field is located in the southern part of the Song Hong basin. Reservoir rocks are carbonates of the Middle Miocene age which developed on an isolated platform (length approximately 100km, and width approximately 15km) on top of Triton Horst structural high.

The Middle Miocene carbonate reservoir is a heterogeneous reservoir with different types of pores: interparticle, vuggy, and fractures with a wide range of porosity from several percent up to over 40% and high variation of permeability, from less than 1mD to over 2000 mD.

The accurate modelling of water saturation is one of the factors that affects the hydrocarbon in place estimation, the prediction of recoverable hydrocarbon, the recovery process, and the future plans for developing such reservoirs. However, the water saturation is not only controlled by the porosity, lithofacies, and other parameters in the Archie formula but also by pore structure, shale content, and wettability that are not consistent in a carbonate reservoir and all of these factors will lead to the high uncertainty in the traditional method for water saturation estimation (Amin et al., 1987; Hamada and Al-Awad, 2001).

Capillary pressure reflects the interaction of

rock and fluids and is controlled by the pore geometry, interfacial tension, and wettability. The capillary pressure concept is an important parameter in volumetric studies where it is used to calculate field wide saturation-height relationships from core and log information (Harrison and Jing, 2001). Capillary pressure can be obtained from Special Core Analysis (SCAL) using the porous plate, centrifuge method, Mercury Injection method, etc.

With Saturation Height Function (SHF), the geologist or reservoir engineer can predict the saturation anywhere in the reservoir for the given height above the free water level (FWL) and for a given reservoir permeability or porosity independently of Archie parameters.

2. Dataset and workflow

The dataset of cores and well logs was taken from the Middle Miocene carbonate reservoir of the CX field. The study dataset included over 1000 core plugs of RCAL; Capillary pressure from 20 porous plates and 132 MICP samples of 3 wells. Figure 1 shows the distribution of K, PHI, FZI, and a cross plot of K versus PHI from RCAL results.

The core data was combined with conventional logging data including GR, LLD, LLS, MSFL, RHOB, NPHI, DTC, and DTS from 3 wells.

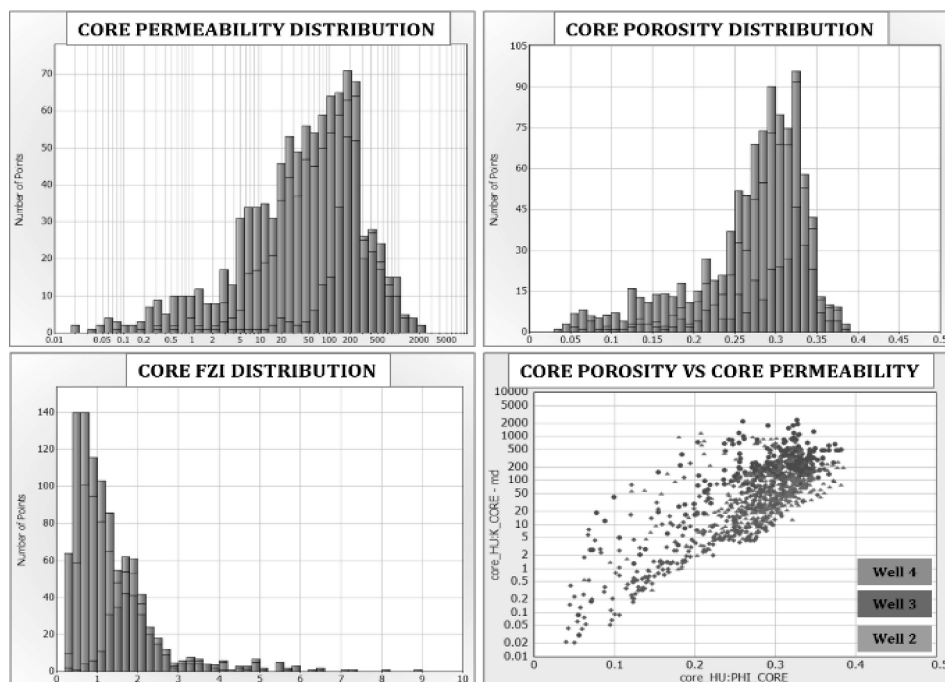


Figure 1. Distribution of core permeability K_{core} , core porosity PHI_{core} , FZI_{core} and crossplot K_{core} vs Phi_{core} of wells in CX field.

The first attempt was done using the universal, normalized saturation curves generated from the Leverett J-function, however, the results show poor behavior due to the heterogeneity of the carbonate reservoir.

To overcome that limitation, the rock typing method using the Hydraulic Flow Unit (HFU) approach was applied. An HFU is defined as that part of the reservoir volume comprising lithologies having reservoir characteristics, along with non-reservoir rocks and the fluids they contain. The flow unit has consistent physical characteristics that control fluid flow which are different from the characteristics of other reservoir volumes (Ebanks, 1987). Each flow unit contains core data and electric log data that can be correlated and mapped between wells.

The HFU was originally introduced by Amaefule et al. (1993) et al. The technique was then developed by many researchers and applied to both carbonate and sandstone reservoirs. In this study, Flow Zone Indicators (FZI) analysis was used as a basis for HFU clustering.

The workflow for water saturation estimation using the Saturation Height Function is as follows:

1. HFU clustering using FZI value;
2. Building SHF for each HFU;

3. Permeability/ HFU prediction from a well log using machine learning;
4. Sw estimation using built SHF for each depth above FWL.

Saturation profiles were created for the Middle Miocene carbonate reservoir and their validity was checked against saturation profiles interpreted from electric logs.

3. Results and Discussion

3.1. HFU classification

Based on over 1.000 core plugs of RCAL from 3 wells in the study area, the FZI value was calculated and then clustered using an unsupervised machine learning technique. A total of 5 HFU was defined as the optimal number using the Elbow method and K_means clustering method (Figure 2). Each HFU has its range of FZI values and the FZI_mean.

3.2. Building SHF for each HFU

A total of 20 Pc curves from the porous plate method and 132 Pc curves from MICP data were collected from the study area. Each data point was

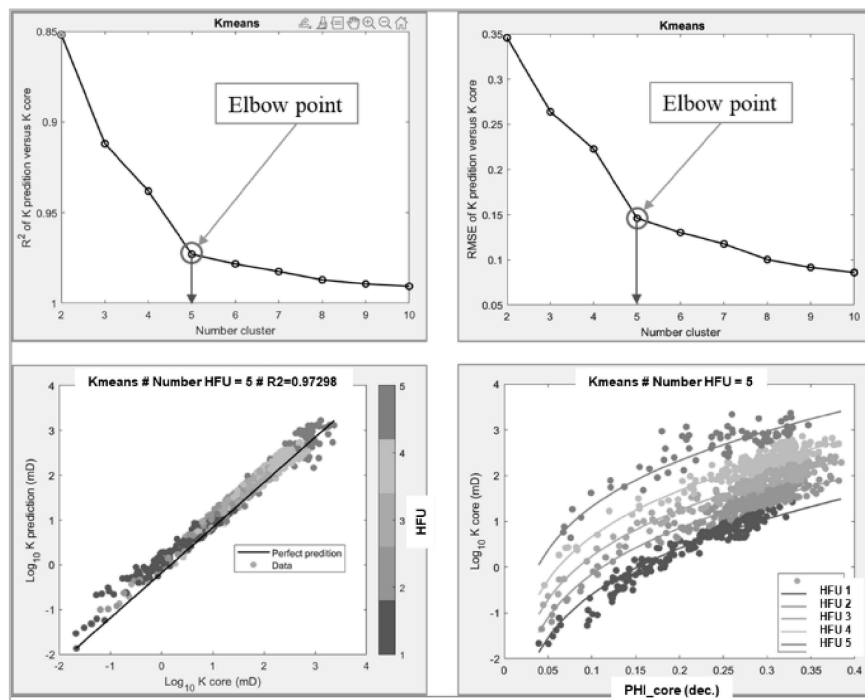


Figure 2. HFU clustering using K-mean method result (K core - core permeability (mD), K prediction - predicted permeability (mD), PHI_{core} - core porosity (dec.).

assigned for the appropriate HFU using the HFU clustering result from the 1st step and plotted over the Sw data (Figure 3).

The field wide SHF can be generated using various practical techniques that relate the capillary pressure curves to reservoir porosity, and permeability for each HFU. The classic method is based on Leverett's J-function approach. Other commonly used methods include Brook Corey, Lambda, Thomeer and Skelt-Harrison. All of the above method was applied for the study area and the Skelt-Harrison method gave the best result with the lowest error (Figures 4a-4e).

Skelt-Harrison method:

The Skelt-Harrison method can be described by the following equation (1):

$$S_w = 1 - A \cdot \exp\left(-\left[\frac{B}{h + D}\right]^C\right) \quad (1)$$

where: Sw - water saturation at capillary pressure; A, B, C, D - the regression constants/ fitting parameters; h - height above Free Water Level (m); Sw - fraction of pore volume.

The strength of Skelt's function is that, rather than linearise the function using exponent, it makes use of its non-linearity to provide a fitted curve shape that actually looks like a capillary pressure curve (Harrison and Jing, 2001).

The models are calculated using the PC_IFT system, assuming that they have the same pore

throat. This transformation of the input SCAL measurements eliminates differences between methods and the liquid systems used, allowing for the comparison of data from different fields in one model on the same scale.

$$P_C = \frac{2 \sigma \cos \theta}{r} \Rightarrow \frac{2}{r} = \frac{P_C}{\sigma \cos \theta} = PC_{IFT} = \frac{P_{C_{RES}}}{\sigma_{RES} \cos \theta_{RES}} = \frac{P_{C_{LAB}}}{\sigma_{LAB} \cos \theta_{LAB}} \quad (2)$$

$$P_{C_{RES}} = P_{C_{LAB}} \cdot \frac{\sigma_{RES} \cos \theta_{RES}}{\sigma_{LAB} \cos \theta_{LAB}}$$

The units are bars for PC, dyne/cm for IFT, and degrees for θ.

The objective of the core build model is to generate modelled capillary pressure curves utilizing petrophysical properties like permeability and porosity.

In the core build model, laboratory data is used to create capillary pressure curves by extrapolating point measurement information.

The best fitting curve for each sample is determined based on the model type. Fitting parameters are defined if they are correlated to petrophysical properties, resulting in a matrix cross-plot that shows three parameters (porosity, permeability, and the square root of permeability/porosity ratio) using the Skelt-Harrison model

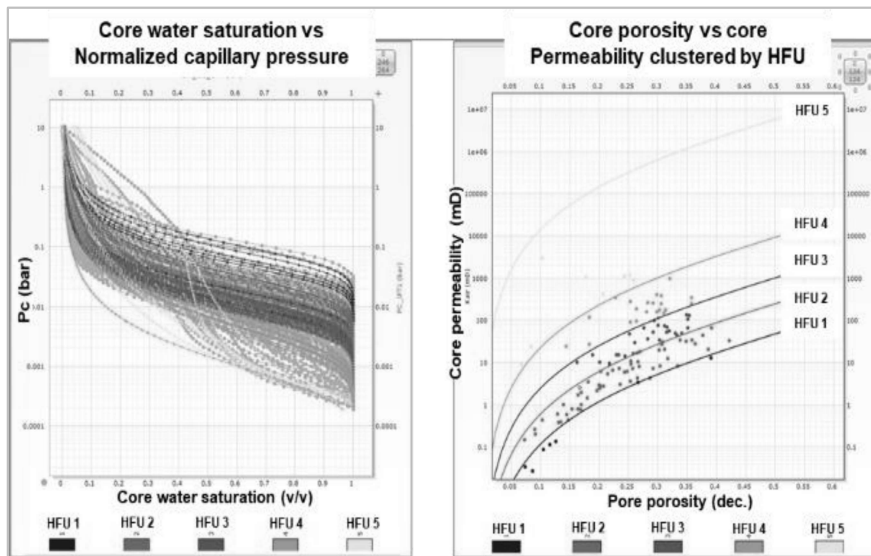


Figure 3. Pc vs Sw for each HFU from study area.

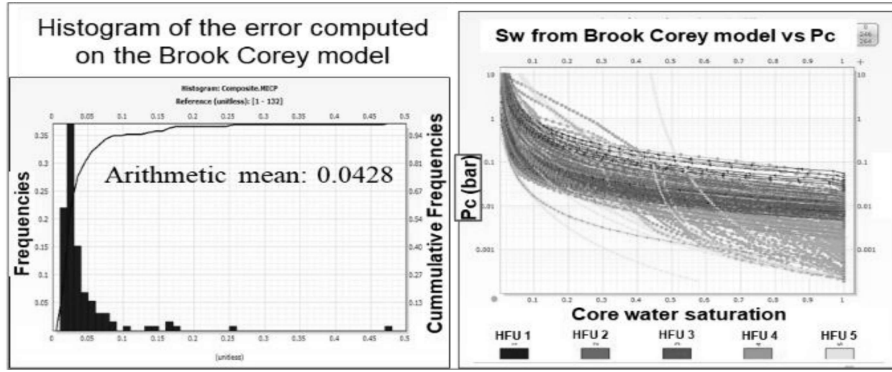


Figure 4a. Histogram of the error computed on the Brook Corey model.

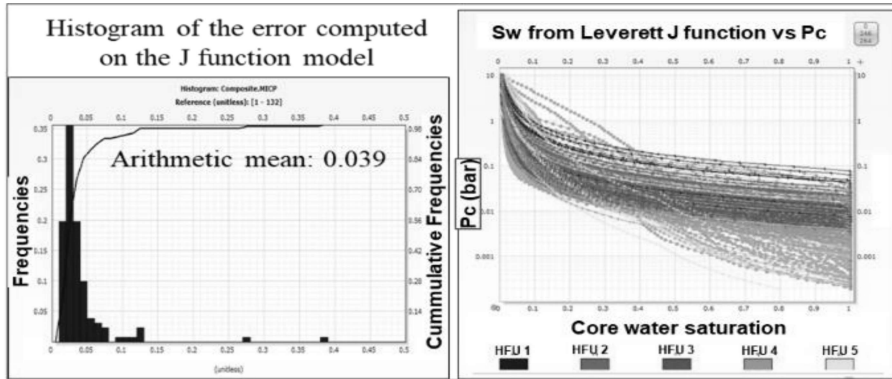


Figure 4b. Histogram of the error computed on the Leverett J function.

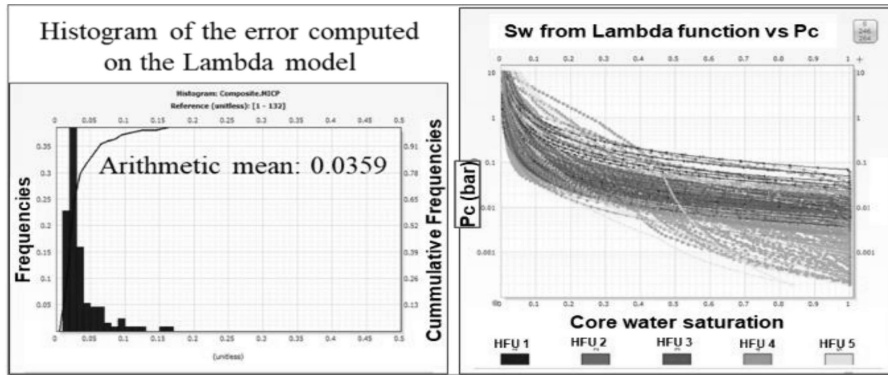


Figure 4c. Histogram of the error computed on the Lambda function.

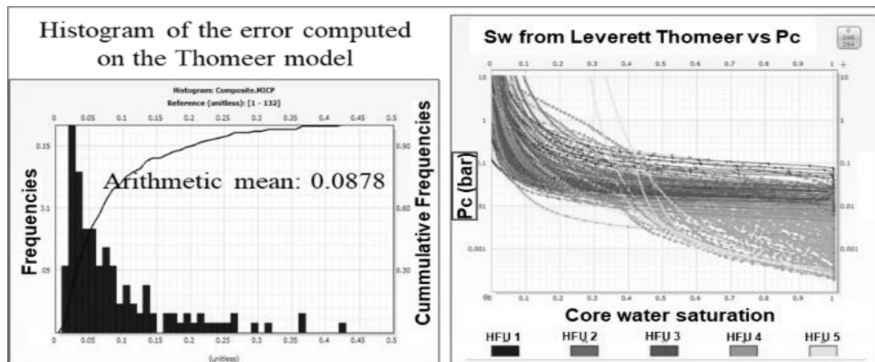


Figure 4d. Histogram of the error computed on the Thomeer model.

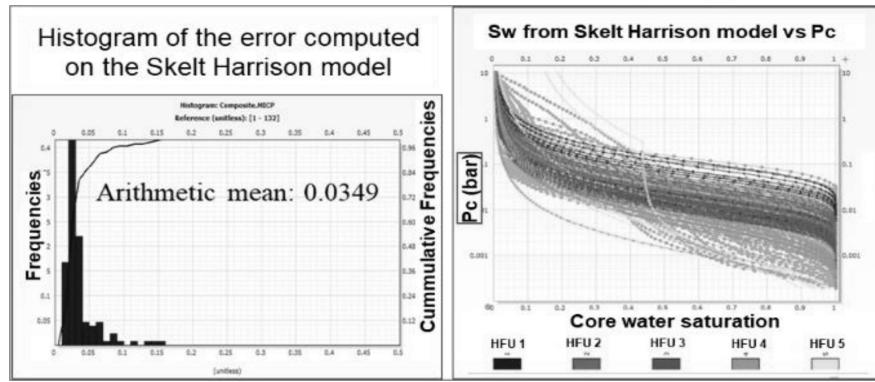


Figure 4e. Histogram of the error computed on the Skelt Harisson model.

The matrix cross-plot comprises nine (9) sub-cross plots, with each containing five types of regression. A total of thirteen (13) possible regressions for each parameter are calculated and the one with the highest determination coefficient (R2) is selected. Using these regression equations and the petrophysical properties of each core sample, new fitting parameters are computed.

The results of the water saturation best fit and capillary model for each HFU using the Skelt Harrison model are shown in the following Figures 5÷9.

The selected parameters using the Skelt Harrison model for HFU 1 are as follows:

- $PC_IFT1 = (HAFWL * (0.98152 - 0.18014) * 0.0980665 * (1.0 / (50 * 1)))$
- $A = 0.994759$
- $B = (0.00279277 * Pow(POR, -1.35963))$
- $C = 1.12355$
- $D = 0$

$$SW = \text{Min}(1, \text{Max}(0, \text{If}((B < 0 \text{ Or } PC_IFT1 \leq -D), 1, 1 - A * \text{Exp}(-\text{Pow}(B / (D + PC_IFT1), C))))))$$

The selected parameters using the Skelt Harrison model for HFU 2 are as follows:

- $PC_IFT1 = (HAFWL * (0.98152 - 0.18014) * 0.0980665 * (1.0 / (50 * 1)))$
- $A = 0.992609$
- $B = (0.0230608 * Pow(PERM, -0.298812))$
- $C = 1.02147$
- $D = 0$

$$SW = \text{Min}(1, \text{Max}(0, \text{If}((B < 0 \text{ Or } PC_IFT1 \leq -D), 1, 1 - A * \text{Exp}(-\text{Pow}(B / (D + PC_IFT1), C))))))$$

The selected parameters using the Skelt Harrison model for HFU 3 are as follows:

- $PC_IFT1 = (HAFWL * (0.98152 - 0.18014) * 0.0980665 * (1.0 / (50 * 1)))$
- $A = 0.992855$

- $B = (0.0252263 - 0.014156 * \text{Log}(\text{Sqrt}(PERM / POR)))$
- $C = 1.00401$
- $D = 0$

$$SW = \text{Min}(1, \text{Max}(0, \text{If}((B < 0 \text{ Or } PC_IFT1 \leq -D), 1, 1 - A * \text{Exp}(-\text{Pow}(B / (D + PC_IFT1), C))))))$$

The selected parameters using the Skelt Harrison model for HFU 4 are as follows:

- $PC_IFT1 = (HAFWL * (0.98152 - 0.18014) * 0.0980665 * (1.0 / (50 * 1)))$
- $A = 0.995728$
- $B = (0.0176328 - 0.00560397 * \text{Log}(PERM))$
- $C = 0.762647$
- $D = 0$

$$SW = \text{Min}(1, \text{Max}(0, \text{If}((B < 0 \text{ Or } PC_IFT1 \leq -D), 1, 1 - A * \text{Exp}(-\text{Pow}(B / (D + PC_IFT1), C))))))$$

The selected parameters using the Skelt Harrison model for HFU 5 are as follows:

- $PC_IFT1 = (HAFWL * (0.98152 - 0.18014) * 0.0980665 * (1.0 / (50 * 1)))$
- $A_PT1 = \text{Pow}(10, -0.490762 - 2.37374 * POR)$
- $\text{Lambda_PT1} = 0.332301$
- $B_PT1 = -0.04702$
- $SWi_PT2 = (0.482889 - 0.098745 * \text{Log}(PERM))$
- $PCe_PT2 = \text{Pow}(10, -3.55136 - 0.000188502 * PERM)$
- $G_PT2 = (0.685344 + 0.000782752 * PERM)$

$$SW = \text{Min}(\text{Min}(1, \text{Max}(0, A_PT1 * \text{Pow}(PC_IFT1, -\text{Lambda_PT1}) + B_PT1)), \text{Min}(1, \text{Max}(0, \text{If}(PC_IFT1 < PCe_PT2, 1, SWi_PT2 + (1 - SWi_PT2) * (1 - \text{Pow}(\text{Exp}(1), (G_PT2 / \text{Ln}(PCe_PT2 / PC_IFT1))))))))))$$

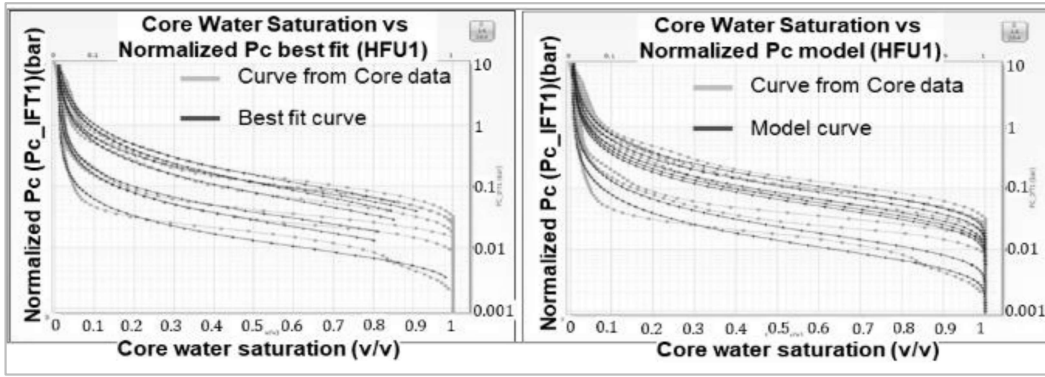


Figure 5. Water saturation best fit and capillary pressure model for HFU 1 using Skelt Harrison model.

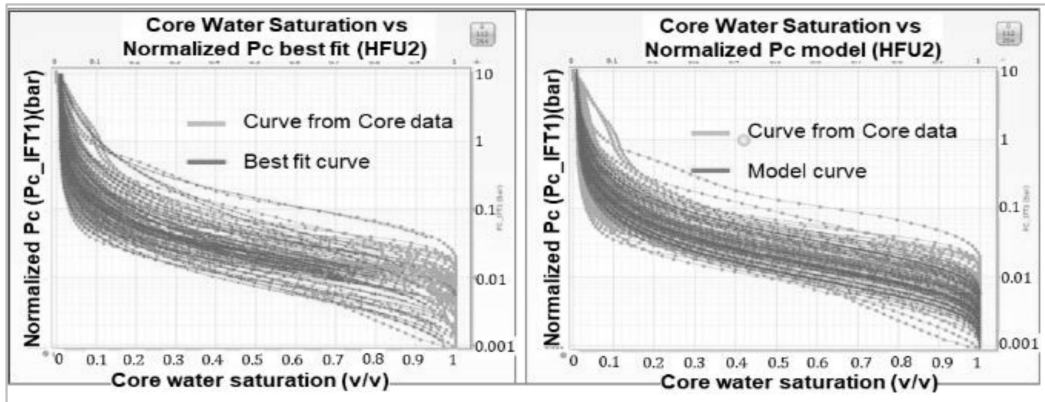


Figure 6. Water saturation best fit and capillary pressure model for HFU 2 using Skelt Harrison model.

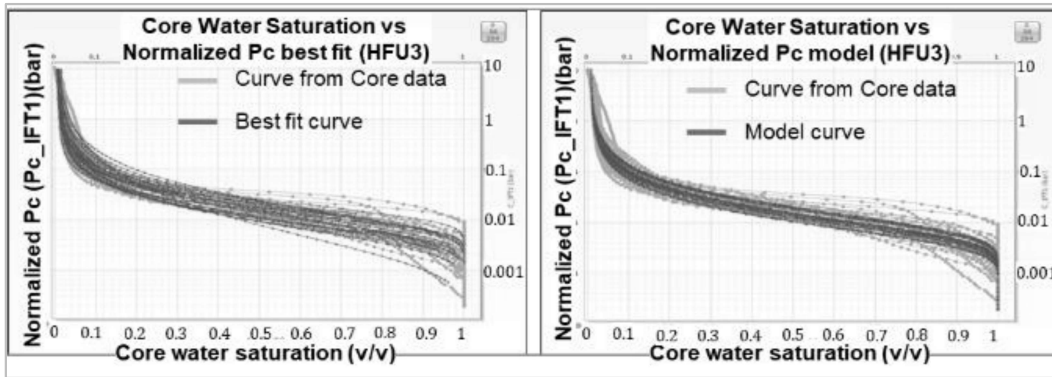


Figure 7. Water saturation best fit and capillary pressure model for HFU 3 using Skelt Harrison model.

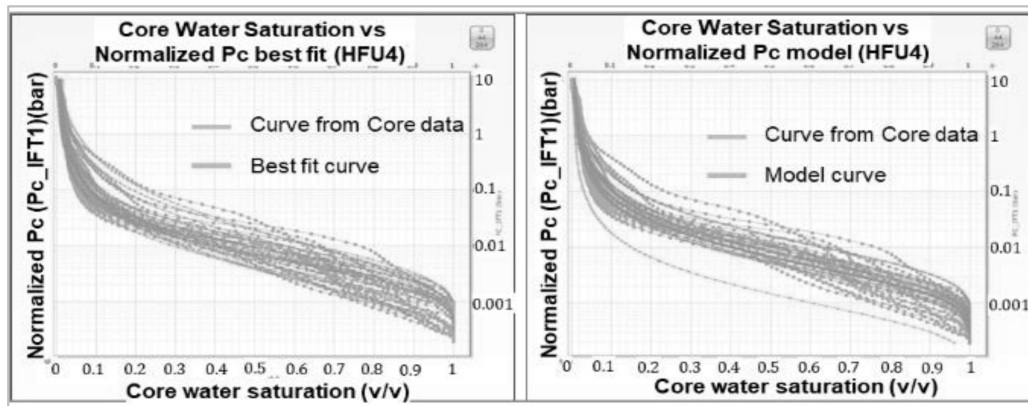


Figure 8. Water saturation best fit and capillary pressure model for HFU 4 using Skelt Harrison model.

3.3. Permeability/ HFU prediction from a well log using machine learning

The permeability prediction from well logs data for uncored sections was performed using various supervised learning models. The correlation coefficient R2 and the RMSE Root Mean Squared Error of these models for both validation data and testing data were compared, and the most appropriate model (Gaussian

Process Regression Exponential) was chosen (Table 1).

The model was then applied to all the carbonate intervals. HFU number for each individual point will be assigned using the FZI value calculated from the predicted permeability and porosity from well logs.

Sw estimation using built SHF for each depth above FWL

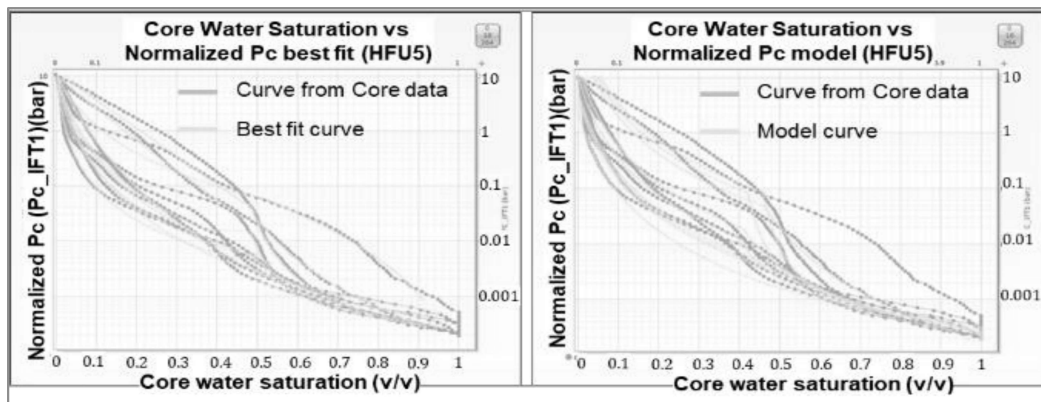


Figure 9. Water saturation best fit and capillary pressure model for HFU 5 using Skelt Harrison model.

Table 1. The training result for permeability prediction using supervised machine learning.

Model Number	Model Type	RMSE		MSE		MAE		RSquared		
		Preset	Validation	Test	Validation	Test	Validation	Test	Validation	Test
1	Linear Regression	Linear	0.516	0.463	0.266	0.215	0.39	0.361	0.679	0.717
2		Interactions	0.504	0.418	0.254	0.175	0.367	0.326	0.693	0.77
3		Robust	0.518	0.459	0.268	0.21	0.389	0.358	0.677	0.723
4		Stepwise	0.512	0.463	0.262	0.214	0.382	0.361	0.684	0.718
5	Tree	Fine	0.481	0.332	0.231	0.11	0.31	0.22	0.722	0.855
6		Medium	0.481	0.355	0.232	0.126	0.332	0.257	0.721	0.834
7		Coarse	0.543	0.437	0.295	0.191	0.384	0.323	0.644	0.749
8	SVM	Linear	0.518	0.461	0.269	0.213	0.39	0.36	0.676	0.72
9		Quadratic	0.489	0.394	0.239	0.155	0.338	0.287	0.712	0.795
10		Cubic	0.614	0.32	0.376	0.103	0.31	0.236	0.546	0.865
11		Fine	0.432	0.282	0.187	0.079	0.269	0.185	0.775	0.896
12		Medium	0.457	0.35	0.209	0.122	0.319	0.261	0.748	0.839
13	Coarse	0.523	0.454	0.274	0.206	0.382	0.341	0.67	0.729	
14	Ensemble	Boosted	0.428	0.343	0.183	0.118	0.306	0.269	0.779	0.845
15		Bagged	0.416	0.287	0.173	0.082	0.279	0.209	0.792	0.892
16	Gaussian Process Regression	Square Exponential	0.416	0.286	0.173	0.082	0.215	0.137	0.791	0.892
17		Matern 5/2	0.361	0.267	0.131	0.071	0.184	0.127	0.843	0.906
18		Exponential	0.329	0.235	0.108	0.055	0.16	0.11	0.87	0.927
19		Rational Quadratic	0.323	0.235	0.105	0.055	0.16	0.112	0.874	0.927
20	Neural Network	Narrow	0.454	0.352	0.206	0.124	0.315	0.267	0.752	0.837
21		Medium	0.452	0.337	0.204	0.113	0.283	0.239	0.754	0.851
22		Wide	0.5	0.341	0.25	0.117	0.267	0.182	0.699	0.846
23		Bilayered	0.449	0.38	0.202	0.145	0.298	0.251	0.757	0.81
24		Trilayered	0.481	0.315	0.232	0.099	0.303	0.216	0.721	0.869

The FWL for each well was defined using pressure data from the RCI/MDT log. The water saturation Sw_{SHF} was estimated using the built SHF for each depth above FWL.

The Sw_{SHF} was checked against the log derived water saturation as there is no other source of water saturation; no direct measurement of Sw from core data is available.

The estimated Sw_{SHF} was plotted against the log-derived water saturation Sw_T (Figure 10)

From the plot, we can see that above the transition zone, the Sw_{SHF} and Sw_T values have many similarities, except for points with low porosity values. The permeability values at these points according to the core sample analysis results can still allow gas to flow (considering gas flow where permeability >0.1 mD), but the Sw_T results are quite high (>0.7), which is quite inappropriate. Thus, the result of estimated Sw_{SHF} in this zone is more optimal than log-derived Sw_T .

In the transition zone, there is a relatively large difference between Sw_{SHF} and Sw_T in well 3 and well 4 (marked brown in track water saturation in Figure 10). The Sw_{SHF} is higher than Sw_T in this zone.

The initial water saturation estimation in transition zones in heterogeneous reservoirs is

long lasting challenge. Due to the lack of knowledge of Archie exponents such as m and especially n value, the log-derived saturation can bear considerable unreliability. Moreover, in the transition zone, True Formation Resistivity evaluation presents a wide range of uncertainties (Zahaf et al., 2014). Therefore, there is a strong need for an independent source of water saturation profile like water saturation from the SHF model.

The water saturation distribution within the transition zone is controlled by the distribution of rock types (by HFU in this study). The height of the transition zone depends on the reservoir rock types. The better the reservoir quality, the thinner the transition zone, and vice versa. With dominant HFU 3 in this zone of wells 3, and 4, the water saturation will change gradually, not change dramatically as Sw_T . So the Sw_{SHF} shows a more reasonable behavior in this zone.

4. Conclusion

The study workflow combines the result of HFU classification, and permeability prediction using machine learning methods into the saturation height function building process.

In the study area, the Skelt Harrison model gave the best result for SHF modeling.

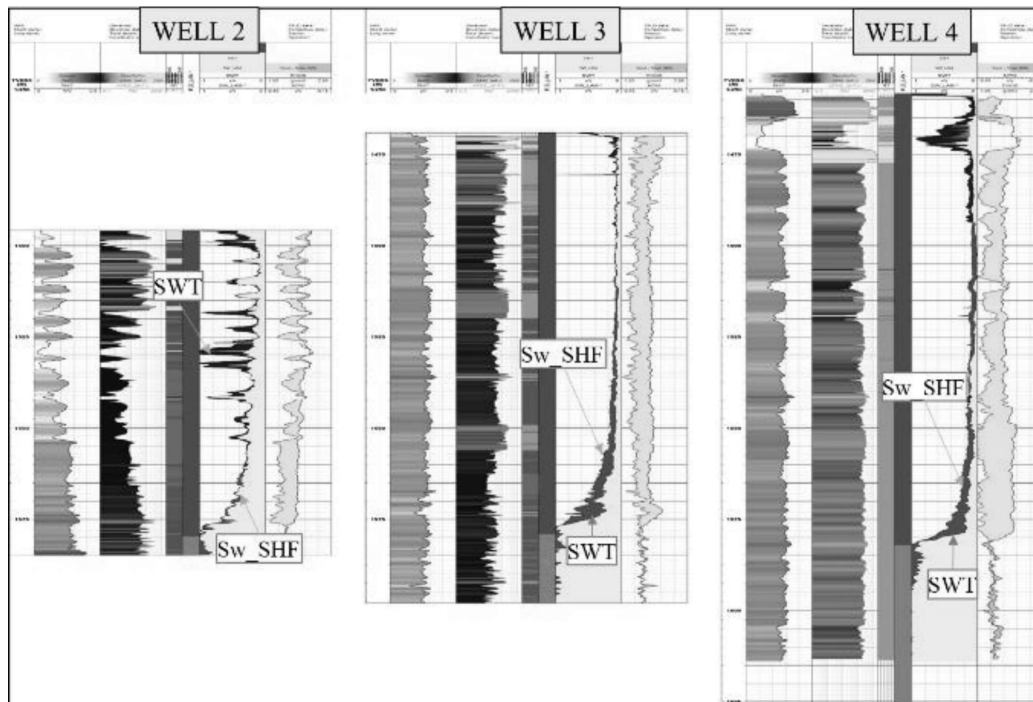


Figure 10. Sw estimation result using SHF model built for 5 HFUs.

The water saturation distribution within the transition zone depends on the distribution of HFU representing the rock qualities. The results of water saturation estimation using SHF differ from log-derived SwT, especially in wells 3 and 4 at the transition zone. The transition zone always exists in the field with water leg, and its thickness depends on rock quality. The Sw_SHF gave a better water profile in this zone over the log-derived water saturation SwT.

The Sw from the SHF model is reliable and can be applied for the whole field with known FWL and porosity-permeability distribution.

Nomenclature

DTC	Compressional sonic log, $\mu\text{s}/\text{ft}$
DTS	Shear sonic log, $\mu\text{s}/\text{ft}$
FZI	Flow Zone Indicator
FWL	Free Water Level
GR	Gamma Ray
K	Permeability, mD
K_core	Core permeability, mD
HFU	Hydraulic Flow Unit
h	Height above free water level, m
LLD	Deep lateral log, ohm.m
LLS	Shallow lateral log, ohm.m
MSFL	Micro Spherical Focus Log, ohm.m
NPHI	Neutron porosity
Pc	Capillary pressure, psi
PHI	Porosity
PHI_core	Core porosity
RCAL	Routine Core Analysis
RHOB	Density log, g/cm^3
SCAL	Special Core Analysis
SHF	Saturation Height Function
SwT	Log-derived water saturation
Sw_SHF	Water saturation estimated from SHF.

Acknowledgment

This research is funded by Vietnam National Foundation for Science and Technology Development (NAFOSTED) under grant number 105.04-2021.23.

Contribution of authors

Dung Trung Nguyen - outline and HFU classification; Man Quang Ha, Hoa Khac Truong - Permeability prediction; Viet Hong Nguyen - Sw estimation; Huong Thien Phan, Cu Minh Hoang - review and conclusion.

References

- Amaefule, J. O., Altunbay, M., Tiab, D., Kersey, D. G., & Keelan, D. K. (1993). Enhanced Reservoir Description: Using Core and Log Data to Identify Hydraulic (Flow) Units and Predict Permeability in Uncored Intervals/Wells. *In Proceedings of the SPE Annual Technical Conference and Exhibition*, Houston, TX, USA, 3-6 October 1993; p. SPE-26436-MS.
- Amin, A. T., Watfa, M., & Awad, M. A. (1987). Accurate estimation of water saturations in complex carbonate reservoirs. *In SPE Middle East Oil and Gas Show and Conference* (pp. SPE-15714). SPE.
- Ebanks, W. J. (1987). Flow unit concept-integrated approach to reservoir description for engineering projects. *AAPG (Am. Assoc. Pet. Geol.) Bull.;*(United States), 71(CONF-870606).
- Hamada, G. M., & Al-Awad, M. N. (2001). Evaluating uncertainty in archie's water saturation equation parameters determination methods. *In SPE Middle East Oil and Gas Show and Conference* (pp. SPE-68083). SPE.
- Harrison, B., & Jing, X. D. (2001). Saturation height methods and their impact on volumetric hydrocarbon in place estimates. *In SPE Annual Technical Conference and Exhibition* (pp. SPE-71326). SPE.
- Zahaf, K., Bourdarot, G., & Low, S. (2014). Water saturation in transition zone in carbonate reservoirs: Reconciling open hole log and capillary pressure. *In Abu Dhabi International Petroleum Exhibition and Conference* (p. D041S070R006). SPE.